Provably Secure Camouflaging Strategy for IC Protection

Meng Li *Student Member, IEEE*, Kaveh Shamsi *Student Member, IEEE*, Travis Meade *Student Member, IEEE*, Zheng Zhao *Student Member, IEEE*, Bei Yu *Member, IEEE*, Yier Jin *Member, IEEE*, David Z. Pan *Fellow, IEEE*

***Abstract*— The advancing of reverse engineering techniques has complicated the efforts in intellectual property protection. Proactive methods have been developed recently, among which layout-level IC Camouflaging is the leading example. However, existing camouflaging methods are rarely supported by provably secure criteria, which further leads to an over-estimation of the security level when countering latest de-camouflaging attacks, e.g., the SAT-based attack. In this paper, a quantitative security criterion is proposed for de-camouflaging complexity measurements and formally analyzed through the demonstration of the equivalence between the existing de-camouflaging strategy and the active learning scheme. Supported by the new security criterion, two camouflaging techniques are proposed, including the low-overhead camouflaging cell generation strategy and the AND-tree camouflaging strategy, to help achieve exponentially increasing security levels at the cost of linearly increasing performance overhead on the circuit under protection. A provably secure camouflaging framework is then developed combining these two techniques. Experimental results using the security criterion show that camouflaged circuits with the proposed framework are of high resilience against different attack schemes with only negligible performance overhead.**

***Index Terms*—IC Camouflaging, SAT-based Attack, Active Learning, Provably Secure, AND-Tree**

I. Introduction

With the increase of IC design costs, intellectual property (IP) privacy and infringement becomes a significant concern for the semiconductor industry. One of the major threats arises from reverse engineering (RE) [1]–[5]. By stripping the integrated circuit (IC) layer by layer, gate-level netlist can be extracted and duplicated without the authorization of the IP holder [4], [6]. To protect IC design against RE, IC camouflaging is proposed as a layout-level technique to hide the circuit functionality [7]–[15]. By synthesizing circuits with logic cells that look alike but can have different functionalities (aka camouflaging cells), the functionality of original circuits cannot be determined from physical RE.

Existing work on IC camouflaging mainly falls into the following three categories: fabrication level [7]–[9], [16], cell level [10], [17]–[20] and gate netlist level [10], [21]. Fabrication-level camouflaging mainly focuses on developing fabrication techniques that can hide the circuit structure. In [7], a doping based technique is proposed. By changing the polarity of dopant for the source and drain of MOS transistors, always-on and always-off transistors can be created. In [8], similar effect is realized by changing the type and length of the Lightly-Doped-Drain (LDD) implants. A dummy contact-based method is also proposed to control the connection between two adjacent layers [9]. By creating gaps in the middle of a contact, two layers that appear to connect are actually disconnected. Both doping-based and contact-based methods are shown to be robust against existing RE techniques [7], [9].

M. Li, Z. Zhao and D. Pan are with the Department of Electrical and Computer Engineering, University of Texas, Austin TX, USA (email: meng_li@utexas.edu, zzhao@utexas.edu, dpan@utexas.edu).

K. Shamsi and Y. Jin are with the Department of Electrical and Computer Engineering, University of Florida, Gainesville, FL, USA (email: kshamsi@ufl.edu, yier.jin@ece.ufl.edu).

T. Meade is with the Department of Computer Science, University of Central Florida, Orlando, FL, USA (email: travm12@knights.ucf.edu).

B. Yu is with the Department of Computer Science and Engineering, The Chinese University of Hong Kong, NT, Hong Kong (email: byu@cse.cuhk.edu.hk).

Cell-level camouflaging leverages the fabrication techniques to build camouflaging cells that look alike but may have different functionalities. In [10], the proposed cell can function as an XOR, NAND or NOR based on the configuration of the true and dummy contact. In [17], [18], by controlling the doping scheme, a camouflaged lookup table (LUT) is created with more than hundreds of functionalities. While these camouflaging cells can hide the real functionality from physical RE, they usually incur large overhead in terms of power, timing and area compared with regular cells. Gate netlist level camouflaging seeks to develop camouflaging cell insertion algorithm to maximize the resilience of the circuit netlist against RE techniques given pre-defined overhead constraints. For example, the authors in [10], [21], [22] insert interfered camouflaging cells or camouflaging connections to prevent RE. In [23]–[25], new low output-corruptibility camouflaging strategies are further proposed to protect the circuit from more advanced RE techniques [26], [27].

Despite the extensive research on IC camouflaging, there are still fundamental problems that have not been properly solved. First, due to the lack of provably secure criteria to guide IC camouflaging, existing netlist-level methods usually tend to over-estimate the provided security level and in fact, have been shown vulnerable to the existing SAT-based de-camouflaging attacks as well as removal attacks based on structural and functional information [26]–[29]. Second, the insertion of camouflaging cells usually leads to large overhead, which places significant limits on their usage in commercial applications.

In this paper, we propose a new criterion, defined as de-camouflaging complexity, to directly quantify the security of the camouflaged netlist. The proposed security criterion is defined as the number of input-output patterns that an attacker has to evaluate to decide the functionality of the original circuit and is formally analyzed by showing the equivalence between SAT-based de-camouflaging attack and the active learning scheme [30]–[32]. The proposed security criterion is independent of how the SAT-based attack is formulated or what type of machine used for the attack. The equivalence also enables us to identify two key factors that determine the security of a camouflaged netlist.

To increase the security level of the camouflaged netlist, we propose two camouflaging strategies targeting at the two identified factors. The first camouflaging strategy is a new low-overhead camouflaging cell generation, which is mainly based on the observation that the overhead of a camouflaging cell depends on its actual functionality in the circuit. We create a specific kind of camouflaging cell that incurs negligible overhead for one functionality, which allows for a large amount of insertion into the netlist and thus, provides better security protection. The second camouflaging strategy leverages the AND-tree structure for better security. We analyze the stand-alone AND-tree structure to verify its induced exponential increase of security level and further identify two important properties, denoted as tree decomposability and input bias, both of which are important to guarantee its effectiveness in general circuits. Combining these two strategies together, an IC camouflaging framework is then proposed to further optimize the camouflaged circuit for better protection against removal attacks. Experimental results demonstrate that the functionality of the camouflaged netlist generated by our framework cannot be resolved by existing de-camouflaging techniques and the overhead is negligible. We

summarize our contributions as follows:

- We investigate a new security criterion to quantify the de-camouflaging complexity and identify two key factors that can help enforce the security criterion in camouflaged netlist.
- We propose two novel camouflaging strategies to increase the two identified factors.
- We develop an IC camouflaging framework combining the two strategies to further protect the camouflaged circuits against removal attacks.
- We verify our proposed security criterion and framework against state-of-the-art de-camouflaging techniques and demonstrate great resilience with negligible overhead.

The rest of the paper is organized as follows. Section II provides a review on existing de-camouflaging attacks and the preliminaries on active learning scheme. Section III formally builds the equivalence between SAT-based de-camouflaging and active learning with key security factors identified. Section IV and Section V describe the camouflaged cell generation strategy and the AND-tree structure. Section VI proposes an IC camouflaging framework. Section VII demonstrates the performance of the proposed camouflaging framework, followed by conclusion in Section VIII.

II. Background

In this section, the reverse engineering (RE) attack model and attack techniques are reviewed. We also talk about the active learning scheme, which lays the foundation for our analysis on de-camouflaging complexity in Section III.

A. Reverse Engineering Attacks

For an attacker, the main target of RE is to extract the original or equivalent circuit with RE techniques. We follow the widely used attack model and assume the attackers have access to the following two components [10]:

- The camouflaged netlist, which can be acquired from physical RE procedure [4]. The attackers can differentiate between a standard cell and a camouflaging cell, but cannot resolve the functionality of the camouflaging cells.
- A functional circuit which can be acquired from the open market and is treated as a black-box circuit.

Given the functional circuit, the attackers cannot directly probe the internal signals of the black-box circuit. Instead, they can select a sequence of input vectors, import them into the black-box circuit through circuit scan chain, query the functional circuit and observe the corresponding outputs. Attackers will infer the correct circuit functionality based on the collected input-output pairs. To explore the input-output patterns, three different methods have been proposed, including brute force attack [10], testing-based attack [10], [33] and SAT-based attack [26]–[28], [34].

Brute force attack proposes to enumerate the possible functionalities for all the camouflaging cells. Then, input vectors are randomly sampled for logic simulation to rule out the false functionalities until the original or equivalent circuit is found. Brute force attack suffers from scalability problem since the attack complexity increases exponentially with respect to the number of camouflaging cells [10]. Testing-based attack targets at one camouflaging gate at a time. For each target gate, input patterns are generated so that the output of all camouflaging gates that *interfere* with the target gate are known, denoted as justification, and a change at the output of the target gate causes changes at circuit primary outputs, denoted as sensitization. Here, two gates are said to interfere if their outputs are connected to the inputs of same gates, or if the output of one gate is connected to the input of the other [10]. However, when the justification and sensitization conditions cannot be satisfied simultaneously, brute force attack has to be leveraged [10]. As shown in [10], by deliberately inserting gates that interfere with each other, the complexity of testing-based attack is no better than the brute force attack.

SAT-based attack is currently the most powerful de-camouflaging attack method. The algorithm starts by treating all the possible circuit functionalities as candidates and collecting them into a set. Then, by iteratively searching the input patterns that can have different outputs for different candidates in the set, denoted as discriminating inputs [26], false functionalities are identified and removed from the set. The process continues until all the functionalities in the set have the same outputs for all input patterns. The most important characteristic of SAT-based attack is that instead of random sampling input patterns from the whole input space, only discriminating input vectors are selected by solving instances of the circuit satisfiability problem. Then, the black box functional circuit is queried to get the corresponding output vector, which are used to rule out the false functionalities.

Since all the attack strategies described above rely on querying the functional circuit, we denote them as query-based attack. Besides the query-based attack, new attack scheme proposed in [29] tries to leverage the structural and functional footprint of the camouflaging strategies to resolve the original circuit functionality. As observed in [29], existing camouflaging strategies [14], [24] that achieve high resilience against SAT-based attack usually suffer from highly biased signal probability for internal circuit nodes, which is not common in real design and thus, can be leveraged to detect camouflaging cells and determine their actual functionality. Therefore, the signal probability skew-based attack can work collaboratively with SAT-based attack. Until now, no camouflaging strategy has systematically demonstrated convincing resilience against both attack schemes. In this paper, we will develop formal analysis for both of the attacks and propose camouflaging strategies that are secure against all the existing attacks.

B. Active Learning Scheme

In this section, we provide basic definitions concerning active learning. For more detailed description, interested readers can refer to [31].

Considering an arbitrary domain X where a concept h is defined to be a subset of points in the domain, a point $x \in X$ can be classified by its membership in concept h, that is, $h(x) = 1$ if $x \in h$, and $h(x) = 0$ otherwise. A concept class H is a set of concepts. For a target concept $t \in H$, a training sample is a pair $(x, t(x))$ consisting of a point x, which is drawn from X following distribution $\mathcal{D}$, and its classification $t(x)$. A concept h is defined to be consistent with a sample $(x, t(x))$ if $h(x) = t(x)$.

The intuition of active learning is to regard learning as a sequential process, so as to choose samples adaptively. Consider a set S of m samples. The classification of some regions of the domain can be determined, which means all concepts in H that are consistent with S will produce same classification for the points in these regions. Active learning scheme seeks to avoid sampling new points from these regions, and instead, samples only from the regions that contain points which can have different classifications for different concepts in H, denoted as region of uncertainty $\mathcal{R}(S)$. By iteratively sampling from $\mathcal{R}(S)$ and updating $\mathcal{R}(S)$ based on the new sample, t can be learned from H. We use the following example to illustrate the concept of active learning.

Example II.1. *Consider a two-dimensional space, and the target t is a set of points lying inside a fixed rectangular in the plane as shown in Fig. 1. Assuming we already have some samples with their classification, $\mathcal{R}(S)$ can then be decided. Consider the three points s_1, s_2 and s_3 in Fig. 1, the label for s_1 and s_2 can already be determined based on existing samples. Therefore, only s_3 can help provide further information to decide the target t from the concept class H.*

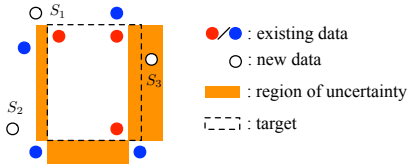

Fig. 1: Example of sampling strategy for active learning.

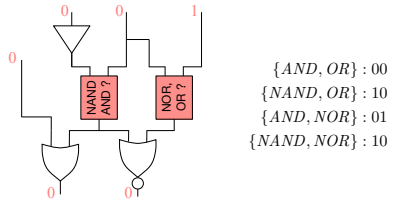

Fig. 2: Example of the camouflaged netlist.

According to [31], if we define error rate $\mathrm{er}_{x\sim\mathcal{D}}(h,t)$ for a concept h with respect to the target t and the distribution $\mathcal{D}$ of points x as $\mathrm{er}_{x\sim\mathcal{D}}(h,t) = \mathsf{Pr}_{x\sim\mathcal{D}}[h(x) \neq t(x)]$, then by adaptively sampling from $x \in X$, to guarantee $\mathrm{er}_{x\sim\mathcal{D}}(h,t) \leq \epsilon$ with sufficient probability, the number of samples m needed for active learning is

$$m = \mathcal{O}(\theta d \log(\frac{1}{\epsilon})),$$

where d is a measure of the capacity of H. Specially, when X is boolean domain with $X = \{0,1\}^n$ and the concept class contains only boolean function, we have $d \geq \dfrac{\log_2|H|}{n}$ [35]. Here $|\cdot|$ denotes the cardinality of the set. θ is the disagreement coefficient, defined as

$$\theta = \sup_\epsilon \frac{\mathsf{Pr}_{x\sim\mathcal{D}}[\mathrm{DIS}(H_\epsilon)]}{\epsilon},$$

where $H_\epsilon = \{h \in H : \mathrm{er}_{x\sim\mathcal{D}}(h,t) \leq \epsilon\}$, and $\mathrm{DIS}(H_\epsilon) = \{x : \exists h, h' \in H_\epsilon \text{ s.t. } h(x) \neq h'(x)\}$, and $\mathsf{Pr}_{x\sim\mathcal{D}}[\mathrm{DIS}(H_\epsilon)] = \mathsf{Pr}_{x\sim\mathcal{D}}[x \in \mathrm{DIS}(H_\epsilon)]$.

III. IC Camouflaging Security Analysis

Let c_o be the original circuit before camouflaging. c_o has n input bits with the input space $I \subseteq \{0,1\}^n$ and l output bits with output space $O \subseteq \{0,1\}^l$. Define the indicator function $e_{c_o} : I \times O \to \{0,1\}$ for c_o, where $I \times O = \{(i,o) : i \in I, o \in O\}$, as

$$e_{c_o}(i,o) = \begin{cases} 1, & \text{if } c_o(i) = o, \\ 0, & \text{otherwise,} \end{cases}$$

where e_{c_o} indicates whether an output vector o can be generated by c_o given certain input vector i.

During the process of IC camouflaging, $\widetilde{m}$ camouflaging gates are inserted into the original netlist, whose functionalities cannot be resolved by physical RE techniques. Let G denote the set of all possible functionalities for the camouflaging gate, where $\forall g \in G$, $g : \{0,1\}^{\widetilde{n}} \to \{0,1\}$ with $\widetilde{n}$ as the input number of the camouflaging gate. Let y denote $\widetilde{m}$ functions chosen from G, i.e. $y \in G^{\widetilde{m}}$, which assigns each camouflaging gate a function in G and let Y denote the set of all possible y. Depending on y, a set of possible circuit functionalities can be created, denoted as C. Note that $c_o \in C$. $\forall c \in C$, there exists a corresponding indicator function e_c. Let E_C denotes the set of indicator functions for all $c \in C$.

Based on the attack model described in Section II, after physical RE, the attacker can acquire the camouflaged netlist but cannot resolve the functionality of the camouflaging cells. Equivalently, the attackers can acquire C and E_C from physical RE. For the attackers, to resolve $c_o \in C$ is equivalent to resolving $e_{c_o} \in E_C$. The attacker can select input pattern $i \in I$, apply to the black-box functional circuit through circuit scan chain and get the correct output $c_o(i)$. Based on $(i, c_o(i))$, all $c \in C$ that are not consistent with $(i, c_o(i))$ can be pruned.

Example III.1. *Consider the camouflaged circuit shown in Fig. 2. We have* $Y = \{\{\mathsf{NAND}, \mathsf{NOR}\}, \{\mathsf{AND}, \mathsf{NOR}\}, \{\mathsf{NAND}, \mathsf{OR}\}, \{\mathsf{AND}, \mathsf{OR}\}\}$. *Assume* $\{\mathsf{AND}, \mathsf{OR}\}$ *gives the correct circuit functionality, then, for input pattern* $\{0001\}$*, by evaluating the black box functional circuit, the correct output vector should be* $\{00\}$*. This indicates* $e_{c_o}(0001, 00) = 1$*. For circuit* c_y *with* $y = \{\mathsf{NAND}, \mathsf{OR}\}$*, given input pattern* $\{0001\}$*, the output becomes* $\{10\}$*, therefore* $e_{c_y}(0001, 10) = 0$*. The indicator functions of the other two functionalities both equal to* 0 *given* $(\{0001\}, \{00\})$*. Therefore, the input-output pattern* $(\{0001\}, \{00\})$ *can help rule out all the false functionalities of the camouflaged circuits.*

To evaluate the effectiveness of camouflaging and the hardness of de-camouflaging, we define the de-camouflaging complexity as the number of input-output patterns required to rule out the false functionalities and resolve $c_o \in C$, equivalently $e_{c_o} \in E_C$. To evaluate the de-camouflaging complexity, we build the equivalence between the SAT-based de-camouflaging strategy and the active learning scheme as follows:

- The set of indicator functions of all possible circuit functionalities E_C corresponds to the concept class H;
- The supply of indicator functions, i.e. $I \times O$, corresponds to the set of points X;
- The indicator function of the original circuit functionality e_{c_o} corresponds to the target concept t;
- The input-output relation $((i, c(i)), 1)$ corresponds to the samples $(x, t(x))$;
- The SAT-based de-camouflaging strategy corresponds to the selective sampling strategy.

Based on the equivalence, the number of input-output patterns required to resolve e_{c_o} with less than ϵ error rate and sufficiently high probability is

$$m(e_{c_o}, E_C) = \mathcal{O}(\theta d \log(\frac{1}{\epsilon})), \tag{1}$$

where $d \geq \frac{\log_2|E_C|}{n}$ is related to the number of functionalities in E_C. θ is calculated as

$$\theta = \sup_\epsilon \frac{\Pr_{(i,o)\sim I\times O}[(i,o) \in \mathrm{DIS}(E_\epsilon)]}{\epsilon}, \tag{2}$$

where $E_\epsilon = \{e_c \in E_C : \mathrm{er}_{(i,o)\sim I\times O}(e_c, e_{c_o}) \leq \epsilon\}$ consists of all the indicator functions that are different from e_{c_o} with probability less than ϵ, and $\mathrm{DIS}(E_\epsilon) = \{(i,o) : \exists e_c, e_{c'} \in E_\epsilon \text{ s.t. } e_c(i,o) \neq e_{c'}(i,o)\}$ consists of all the input-output pairs (i,o) that leads to different outputs of any pair of indicator functions in E_ϵ. We use the following example to illustrate the E_ϵ and $\mathrm{DIS}(E_\epsilon)$.

Example III.2. *Consider the camouflaged circuit and the truth table of all the possible functionalities of the camouflaged circuit shown in Fig. 3. The correct functionality is* c_0 *with* $y^* = \{\mathsf{BUF}, \mathsf{BUF}\}$*. Then, for* c_0*, the indicator function* e_{c_0} *becomes*

$$e_{c_0}(i,o) = \begin{cases} 1, & \textit{if } (i,o) \in \{(00,0),(01,0),(10,0),(11,1)\}, \\ 0, & \textit{otherwise.} \end{cases}$$

Similarly, we can define e_{c_i} *for* c_i*,* $1 \leq i \leq 3$*.* e_{c_1} *has different outputs compared with* e_{c_0} *at four input-output pairs, i.e.* $\{(10,0),(10,1),(11,0),(11,1)\}$*. If we assume* (i,o) *follows a uniform distribution, then* $\mathrm{er}_{(i,o)\sim I\times O}(e_{c_0}, e_{c_1}) = 4/8 = 1/2$*. Similarly, we have* $\mathrm{er}_{(i,o)\sim I\times O}(e_{c_0}, e_{c_2}) = \mathrm{er}_{(i,o)\sim I\times O}(e_{c_0}, e_{c_2}) = 1/2$*. If we set* $\epsilon = 1/2$*,* $E_{1/2} = \{e_{c_0}, e_{c_1}, e_{c_2}, e_{c_3}\}$*. We can also determine* $\mathrm{DIS}(E_{1/2}) = \{(00,0),(00,1),(01,0),(01,1),(10,0),(10,1),(11,1),(11,1)\}$*, and*

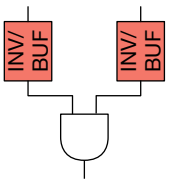

Input	c_0	c_1	c_2	c_3
00	0	0	0	1
01	0	0	1	0
10	0	1	0	0
11	1	0	0	0

Fig. 3: Example of camouflaged netlist and the truth table for all the possible functionalities.

$\Pr_{(i,o)\sim I\times O}[(i,o) \in \mathrm{DIS}(E_{1/2})] = 1$. *By trying different* ϵ*, we know* θ *get the maximum value, i.e.* 2*, when* $\epsilon = 1/2$.

Based on the equivalence of SAT-based attack and active learning, we can identify two key factors that impact the security of different camouflaging strategies, i.e. d and θ, and also use Equation (1) as a quantitative security evaluation metric. It should be noted that Equation (1) refers to a specific scenario defined as Probably Approximately Correct (PAC) learning, which indicates the output of active learning scheme is an approximation of the original functionality with certain probability. However, SAT-based attack is an exact learning scheme. Though different, the exact learning problem is at least as difficult as the PAC learning problem, which indicates Equation (1) can still work as a lower bound of the complexity of the SAT-based attack. In fact, exact learning may not always be necessary. From the attacker's perspective, it is sufficient if he can resolve a circuit functionality, whose output error probability is limited to certain small threshold compared with original circuit functionality. We regard this as a future research direction. In the following sections, we will propose camouflaging techniques to increase d and θ to enhance the resilience against SAT-based attack.

IV. Novel Camouflaging Cell Design

In this section, we target at increasing d as in Equation (1). Because the lower bound of d is in proportional to $|C|$, i.e. $|E_C|$, we choose to increase the number of possible functionalities of the camouflaged netlist. $|E_C|$ is related to the number of camouflaging cells inserted into the circuits, the locations of inserted cells, and the number of possible functionalities of different camouflaging cells. Traditional camouflaging cell generation strategies usually target at increasing the possible functionalities for each cell. However, they usually cause large overheads in terms of power, area and timing, which significantly limits the number of camouflaging cell that can be inserted into the original netlists, and thus, limits the total number of possible functionalities of the camouflaged netlists. We observe that *the overhead of one camouflaging cell is mainly determined by its actual functionality in the circuit.* In this section, we will propose two different camouflaging cell designs, termed as XOR-type cells and stuck-at-fault-type (STF-type) cells, which incur negligible overhead for some specific functionality. As we will show, the proposed designs allow much richer functionalities for the camouflaged netlist with negligible overhead.

A. XOR-type Cell Camouflaging Strategy

The XOR-type camouflaging strategy leverages the dummy contact technique. For example, as shown in Fig. 4(a), for a BUF cell, we modify the shape of the polysilicon to create extra overlap between polysilicon and metal layer. Then, we can configure the functionality of the camouflaging cell by determining whether the five contacts are real or dummy. When contact A, B, D, E are real while contact C is dummy, the cell functions as a BUF. If contact C is real while the rest of the contacts are dummy, the cell functions as an INV. Similar strategy can be applied to other cells including AND, OR and so on.

To evaluate the overhead of the XOR-type camouflaged cells, standard cells from NanGate 45nm Open Cell Library [36] are modified according to the strategy and scaled to 16nm technology. Then Calibre xRC [37] is used to extract parasitic information of the cell layouts. We use SPICE simulation to characterize different types of gates, which are based on 16nm PTM model [38]. As we can see from TABLE I, when the cell functions as a BUF, the overhead induced by the layout modification is negligible compared with original standard cells. However, when the cell functions as an INV, large overhead can be observed for timing, area and power.

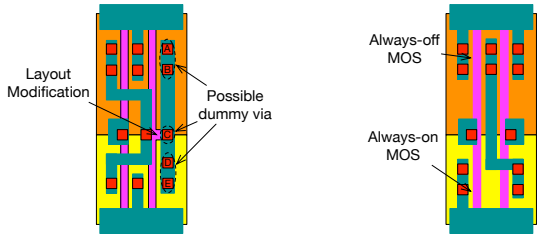

(a) (b)

Fig. 4: Examples of two different cell camouflaging strategies: (a) XOR-type and (b) STF-type.

TABLE I: Overhead characterization of XOR-type camouflaged cell.

Cell	BUF		AND2		OR2		AND3	
Func.	BUF	INV	AND2	NAND2	OR2	NOR2	AND3	NAND3
Timing	1.0×	2.0×	1.0×	1.5×	1.0×	1.9×	1.0×	1.8×
Area	1.0×	1.5×	1.0×	1.3×	1.0×	1.3×	1.0×	1.3×
Power	1.0×	1.5×	1.0×	0.9×	1.0×	1.1×	1.0×	1.0×

B. STF-type Cell Camouflaging Strategy

The STF-type camouflaging strategy leverages the doping-based camouflaging technique. The camouflaging cell generated with the STF-type strategy has exactly the same metal and polysilicon layer compared with the existing standard cells in the library. The only difference comes from the type and the shape of the Lightly-Doped-Drain (LDD), which makes it very difficult to distinguish a regular MOS transistor with the Always-on and Always-off MOS transistor. The STF-type camouflaging strategy fully leverages this flexibility to create camouflaging cells with different functionalities.

For example, as shown in Fig. 4(b), for a NAND2 cell, if we change the doping scheme following [7], we can create Always-on NMOS transistor and Always-off PMOS transistor associated with A. This is equivalent to creating a stuck-at-1 fault at input A and the functionality of the NAND cell becomes an INV for input B. Similar strategy can be applied to all the other cells in the original library. In terms of overhead, it is obvious that the STF-type camouflaging strategy does not impact the timing or performance when it functions normally since the layout is not modified. However, when Always-on or Always-off scheme is used, the overhead needs to be characterized. We use the same method as described for the XOR-type camouflaging strategy and the overhead results is listed in TABLE II.

TABLE II: Overhead characterization of STF-type camouflaged cell.

Cell	OR2		NAND2		AND3		
Func.	OR2	BUF	NAND2	INV	AND3	AND2	BUF
Timing	1.0×	1.4×	1.0×	1.6×	1.0×	1.3×	1.8×
Area	1.0×	1.3×	1.0×	1.5×	1.0×	1.3×	1.7×
Power	1.0×	1.2×	1.0×	1.5×	1.0×	1.1×	1.3×

C. Discussion

As described above, both XOR-type and STF-type camouflaging cells proposed above incur negligible overhead for some specific functionalities. It should be noted that they also have different characteristics. For the XOR-type camouflaging cell, when the attacker mis-interprets the type of the contact, the probability of logic error at the output of the cell is always 1. For the STF-type cell, a mis-interpretation of the doping

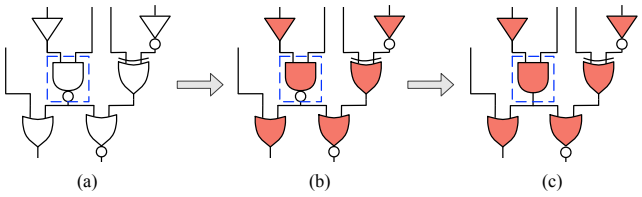

Fig. 5: Two-step IC camouflaging with XOR-type and STF-type cells: (a) original circuit netlist; (b) change all standard cells into camouflaging cells that appear to be same and have same functionalities; (c) random select cells and replace them with cells that appear to be different but work with the same functionalities.

scheme may not always lead to incorrect logic value at the output of the gate. For example, consider an AND gate with $\widetilde{n}$ inputs, denoted as $i_1, i_2, \ldots, i_{\widetilde{n}}$, and first $\widetilde{n}'$ inputs are dummy. Then, the probability of logic error at the output of the cell can be calculated as

$$P_e = \Pr_{i\sim I}\left[\left(\bigcup_{k\in[\widetilde{n}']} i_k = 0\right) \cap \left(\bigcap_{k\in[\widetilde{n}]\setminus[\widetilde{n}']} i_k = 1\right)\right],$$

where $[\widetilde{n}] = \{1, 2, \ldots, \widetilde{n}\}$.

Meanwhile, for the STF-type camouflaging cell, since it is equivalent to creating a stuck-at fault at several input pins of the cell, these input pins become dummy as their logic values do not impact the output of the cell. This enables us to create dummy wire connections between different nodes that are not connected in the original circuit, which not only hides the original functionality, but also hides the circuit structure.

To leverage the XOR-type and STF-type cells to camouflage the original circuits, we propose a two-step strategy. In the first step, we replace all the standard cells with the camouflaging cells, e.g. NAND cell to an STF-type NAND cell in Fig. 5(b). For these camouflaging cells, they are set to work as the cells that they appear to be, e.g. an STF-type NAND cell works as a real NAND gate, and therefore, the replacement incurs negligible overhead based on our characterization results above. Then, in the second step, we randomly choose a small subset of gates in the netlist, and replace them with new camouflaging cells that appear differently but indeed work with the same functionality as the original cells, e.g. a NAND cell is replaced by an XOR-type AND cell in Fig. 5(c). Although overhead can be introduced in the second step, we argue such overhead can be negligible since only a small subset of gates are modified in the second step. Even if we assume the attackers know the number of cells that are changed in the second step, they cannot determine which cells are changed. Therefore, the attacker still cannot determine the functionality for each cell in the camouflaged circuits. With the increase of circuit size, the total number of possible functionalities of the camouflaged netlist also increases, and thus, results in high resilience towards SAT-based attack as shown in our experimental results.

The effectiveness of the proposed camouflaging cell generation strategy is verified in Section VII. However, there are several drawbacks if we simply use the cell generation strategy to protect the circuits:

- Evaluating $|C|$ or $|E_C|$ accurately is computational intractable, which makes it hard to provide provably secure guarantee.
- The effectiveness is limited by the circuit size since we only replace original cells in the original circuits. Empirically, the proposed strategy works well for large circuits but for small circuits, the security is not sufficient.
- Even for large circuit, it is hard to protect all the circuit outputs [21].

To overcome these problems, in Section V, we will propose another camouflaging technique based on AND-tree structure, which provides provably secure guarantee.

V. AND-Tree Camouflaging Strategy

In this section, we target at increasing θ as in Equation (1). In [27], the AND-tree structure is noticed to achieve good resilience to SAT-based de-camouflaging attack when the input pins are camouflaged as shown in Fig. 6. In this section, we provide formal analysis for the AND-tree structure and further identify two important characteristics of the AND-tree structure, denoted as input bias and tree decomposability, to characterize its effectiveness in general circuits.

A. Security Analysis of the AND-Tree Structure

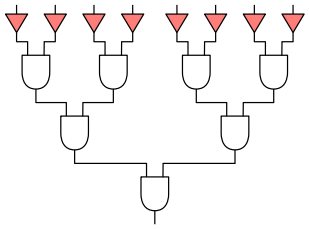

Fig. 6: Example of a camouflaged AND-tree structure.

Consider the AND-tree structure with n input pins shown in Fig. 6, where all the input pins are camouflaged with the XOR-type camouflaging BUF cell. Recall from Section III that $I \subseteq \{0,1\}^n$ and $Y \subseteq G^n$ represent all the possible combinations of functionalities for the camouflaging cells. For any $i \in I$ and $y \in Y$, the output of the AND-tree structure can be expressed as

$$c_y(i) = g_1(i_1) \wedge g_2(i_2) \wedge \ldots \wedge g_n(i_n),$$

where i_k denotes the kth entry of input i, and $g_k(\cdot)$ denotes functionality of the kth camouflaging cell. $g_k(i_k) = i_k$ if the kth cell functions as a buffer, while $g_k(i_k) = \overline{i_k}$ if the kth cell functions as an inverter.

Let $y^* \in Y$ denote the correct configuration for all the camouflaging cells. Then, depending on y, there are 2^n different circuit functionalities, i.e. $|C| = |E_C| = 2^n$. For any $y \in Y$, there exists exactly one input $i \in I$ such that $c_y(i) = 1$, denoted as i^y. Therefore, we have $\Pr_{i\sim I}[c_y(i) = 1] = \Pr_{i\sim I}[i = i^y]$. Now, we have the following lemma for the camouflaged AND-tree structure.

Lemma V.1. *For an n-bit AND-tree structure with all tree inputs camouflaged with XOR-type camouflaging BUF cells, if the logic values for tree inputs follow identical independent Bernoulli distribution with probability of 0.5, then, we have $\theta = 2^{n-1}$.*

To prove Lemma V.1, we will first demonstrate that when the logic value for all the tree inputs follow identical independent Bernoulli distribution with probability of 0.5, for any $y \neq y^*$, the error rate of the indicator function e_{c_y} is $1/2^{n-1}$ compared with $e_{c_{y^*}}$. Meanwhile, we will show that $\mathrm{DIS}(E_\epsilon) = I \times O$. Then, based on the definition of θ in Equation (2), we will prove that $\theta = 2^{n-1}$.

Proof. For any $y \neq y^*$, c_y is different compared with c_{y^*} for exactly two input vectors, i.e. i^y and i^{y^*}. For i^y, because $c_y(i^y) = 1$ while $c_{y^*}(i^y) = 0$, we have $e_{c_y}(i^y, 1) \neq e_{c_{y^*}}(i^y, 1)$ and $e_{c_y}(i^y, 0) \neq e_{c_{y^*}}(i^y, 0)$. Therefore, e_{c_y} has different outputs compared with $e_{c_{y^*}}$ at exactly four points, i.e. $\{(i^y, 1), (i^y, 0), (i^{y^*}, 1), (i^{y^*}, 0)\}$. This indicates $\forall e_{c_y} \in E_C$ with $y \neq y^*$,

$$\begin{aligned}
&\mathrm{er}_{(i,o)\sim I\times O}(e_{c_y}, e_{c_{y^*}}) \\
&= \Pr_{(i,o)\sim I\times O}[e_{c_y}(i,o) \neq e_{c_{y^*}}(i,o)] \\
&= \Pr_{(i,o)\sim I\times O}[(i,o) \in \{(i^y,0),(i^y,1),(i^{y^*},0),(i^{y^*},1)\}] \\
&= \Pr_{i\sim I}[i = i^y \vee i = i^{y^*}] = \Pr_{i\sim I}[i = i^y] + \Pr_{i\sim I}[i = i^{y^*}]. \qquad (3)
\end{aligned}$$

Note when $y = y^*$, $\text{er}_{(i,o)\sim I\times O}(e_{c_y}, e_{c_{y^*}}) = 0$. Therefore,

$$\begin{aligned} E_\epsilon &= \{e_{c_y} \in E_C : \text{er}_{(i,o)\sim I\times O}(e_{c_y}, e_{c_{y^*}}) \le \epsilon\} \\ &= \{e_{c_y} \in E_C : \Pr_{i\sim I}[i = i^y] + \Pr_{i\sim I}[i = i^{y^*}] \le \epsilon\} \cup \{e_{c_{y^*}}\} \\ &= \{e_{c_y} \in E_C : \Pr_{i\sim I}[i = i^y] \le \epsilon - \Pr_{i\sim I}[i = i^{y^*}]\} \cup \{e_{c_{y^*}}\}. \end{aligned} \tag{4}$$

Because $\forall e_{c_y} \in E_\epsilon$, where $y \neq y^*$, is different from $e_{c_{y^*}}$ at exactly four points, we have

$$\begin{aligned} \text{DIS}(E_\epsilon) =& \{(i,o) \in I \times O : \Pr_{i\sim I}[i = i^y] \le \epsilon - \Pr_{i\sim I}[i = i^{y^*}], \\ & o \in \{0,1\}\} \cup \{(i^{y^*}, 1), (i^{y^*}, 0)\}. \end{aligned} \tag{5}$$

For tree inputs, if the logic values follow independent Bernoulli distribution with probability of 0.5, $\forall i^y \in I$, we have

$$\Pr_{(i,o)\sim I\times O}[(i,o) \in \{(i^y, 0), (i^y, 1)\}] = \Pr_{i\sim I}[i = i^y] = \frac{1}{2^n},$$

and $\forall e_{c_y} \in E_C$ with $y \neq y^*$,

$$\text{er}_{(i,o)\sim I\times O}(e_{c_y}, e_{c_{y^*}}) = \frac{1}{2^{n-1}}.$$

Therefore, by setting $\epsilon = 1/2^{n-1}$, we have $E_\epsilon = E_C$ and $\text{DIS}(E_\epsilon) = I \times O$. According to the definition of θ,

$$\theta = \frac{\Pr_{(i,o)\sim I\times O}[(i,o) \in \text{DIS}(E_\epsilon)]}{\epsilon} = 2^{n-1}.$$

Hence proved. □

Base on Lemma V.1, we now have the following theorem concerning the security of a camouflaged AND-tree structure.

Theorem V.2. *For an n-input AND-tree structure with all tree inputs camouflaged with XOR-type camouflaging BUF cells, if the logic values for tree inputs follow identical independent Bernoulli distribution with probability of 0.5, then,*

$$m(e_{c_{y^*}}, E_C) = \mathcal{O}(2^n).$$

Proof. Based on Lemma V.1, we have $\theta = 2^{n-1}$ for an n-input AND-tree. Meanwhile, because $|E_C| = 2^n$, we have $d \ge \log_2 |E_C|/n = 1$. Therefore, $m(e_{c_{y^*}}, E_C) = \mathcal{O}(2^n)$. Hence proved. □

From Theorem V.2, under the assumption that the logic values for tree inputs follow identical independent Bernoulli distribution with probability of 0.5, we can formally prove the security of an n-input AND-tree by showing that the de-camouflaging complexity of a SAT-based attack scales exponentially with the increase of tree input size.

B. AND-Tree Structure in General Circuits

According to the analysis above, a stand-alone AND-tree structure can lead to exponential increase of de-camouflaging complexity. However, this may not be true for an AND-tree structure in general circuits due to the following reasons:

- The input pins to the AND-tree structure may not be primary inputs to the circuit. As shown in Fig. 7(a), since the fanin cone of different input pins can be overlapped, the requirement on independence may not be satisfied. Meanwhile, depending on the logic gates in the fanin cone, the signal probability for each tree input may also deviate from 0.5.
- There are usually more than one primary outputs in the circuit and more than one paths from some internal nodes of an AND-tree to the primary outputs. Consider the AND-tree structure in Fig. 7(b). The internal node $Node_1$ can bypass the root of the tree PO_2 and get observed at the primary output PO_1. This can also reduce the de-camouflaging complexity of the AND-tree structure.

Therefore, to determine the security of an AND-tree structure in general circuits, we need to characterize the two factors, which we define as input bias and tree decomposability.

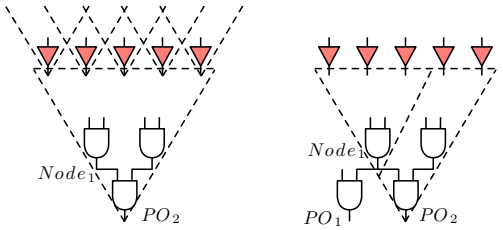

Fig. 7: Two situations that can impact the security of AND-tree structure: (a) overlapped fanin cone for input pins leads to correlation; (b) extra path to primary outputs from internal node makes it possible to decompose the tree.

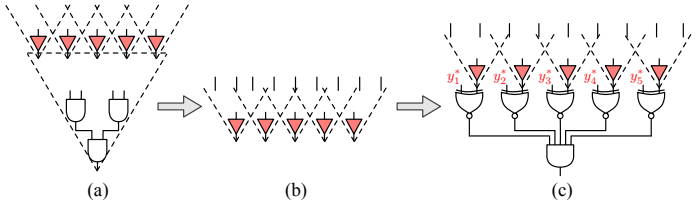

Fig. 8: Exact calculation of $\Pr_{i\sim I}[f_{y^*}(i) = 1]$: (a) original tree structure; (b) fanin cone extracted for all the tree input pins; (c) form the circuit that connects all tree input pins to the desired logic values, i.e. $\{y_1^*, y_2^*, y_3^*, y_4^*, y_5^*\}$. By forcing the output of the formed circuit to 1, we can solve the logic values for the circuit primary inputs iteratively as in Algorithm 1.

1) Input Bias Evaluation

Input bias is proposed to characterize the distance between actual joint distribution for logic values at tree input pins and the ideal independent Bernoulli distribution.

As shown in Fig. 7(a), the logic value of input pins is determined by the primary inputs and logic gates in the fanin cones, which makes the original assumption on independent Bernoulli distribution for input pins invalid. We denote this as input bias since the actual input distribution deviates from the ideal distribution. Input bias mainly impact E_ϵ and $\text{DIS}(E_\epsilon)$. According to Equation (5), to decide $\text{DIS}(E_\epsilon)$, we need to calculate the probability of each input vector, which, however, is intractable for large circuits. To capture the impact of input bias, we instead consider the following approximate approach.

According to Equation (3), $\forall y \neq y^*$, we have

$$\text{er}_{(i,o)\sim I\times O}(e_{c_y}, e_{c_{y^*}}) = \Pr_{i\sim I}[i = i^y] + \Pr_{i\sim I}[i = i^{y^*}] \ge \Pr_{i\sim I}[i = i^{y^*}].$$

To get a non-empty E_ϵ, we must choose $\epsilon \ge \Pr_{i\sim I}[i = i^{y^*}]$. Because we always have $\Pr_{(i,o)\sim I\times O}[(i,o) \in \text{DIS}(E_\epsilon)] \le 1$, then

$$\theta = \frac{\Pr_{(i,o)\sim I\times O}[(i,o) \in \text{DIS}(E_\epsilon)]}{\epsilon} \le \frac{1}{\Pr_{i\sim I}[i = i^{y^*}]}.$$

Therefore, to evaluate the impact of input bias, we can first calculate $\Pr_{i\sim I}[i = i^{y^*}]$ to get the upper bound of θ. If the upper bound is smaller than the pre-defined requirement, then, we conclude the AND-tree in the circuit is not enough to guarantee the security.

To evaluate $\Pr_{i\sim I}[i = i^{y^*}]$, we consider the procedure as shown in Fig. 8. We first extract the fanin cone for all the tree input pins as in Fig. 8(b). Then, as in Fig. 8(c), we form the circuit that connects each tree input pin to its desired logic value. The output of the formed circuit equals to 1 if and only if the logic values for all the tree inputs equal to y^*. Therefore, if we force the output equals to 1 and solve the value for the circuit primary inputs, we can get $\Pr_{i\sim I}[i = i^{y^*}]$. We formulate the problem into a SAT problem and show the pseudo code

in Algorithm 1. FORMSATPROB grabs the fanin cone for the tree input pins and form the SAT equation as in Fig. 8(c) (line 1). Cnt is used to count the total number of input vectors that satisfy the SAT equation, which in turn can be used to calculate $\Pr_{i\sim I}[i = i^{y^*}]$. We initialize Cnt to 0 and iteratively solve the SAT problem to search for the input vectors until the SAT problem is not satisfiable. As we have discussed, to guarantee security, $\Pr_{i\sim I}[i = i^{y^*}]$ cannot be larger than a threshold. This enables us to set a threshold for the maximum value of Cnt, i.e T_h in line 6. The efficiency highly depends on the $\Pr_{i\sim I}[i = i^{y^*}]$ as it determines the iterations of the algorithm. Because to guarantee the security level, $\Pr_{i\sim I}[i = i^{y^*}]$ is usually small, the overall efficiency of the algorithm is quite acceptable.

Algorithm 1 Algorithm of Calculating $\Pr_{i\sim I}[i = i^{y^*}]$

1: $F \leftarrow$ FORMSATPROB(G, i, y, y^*);
2: $Cnt \leftarrow 0$;
3: **while** F is satisfiable **do**
4: $\quad i_t \leftarrow$ SATSOLVE(F);
5: $\quad Cnt \leftarrow Cnt + 1$;
6: $\quad$ **if** $\frac{Cnt}{2^{|i|}} \geq T_h$ **then**
7: $\quad\quad$ **Return** $\frac{Cnt}{2^{|i|}}$;
8: $\quad F \leftarrow F \wedge (i \neq i_t)$;
9: **Return** $\frac{Cnt}{2^{|i|}}$;

Given $\Pr_{i\sim I}[i = i^{y^*}]$, we can determine the upper bound of the de-camouflaging complexity for the tree structure. When the upper bound is large enough, to further evaluate the tree structure, we calculate the distance between the actual distribution for logic values of tree input pins compared with the ideal distribution. Our intuition is that while the ideal distribution provides the best security, the closer the actual distribution is compared to the ideal distribution, the better security the tree structure can provide. To evaluate the distance between different distributions, we adopt the normalized Kullback-Leibler (KL) divergence [39].

Normalized KL divergence for two discrete probability distribution, P and Q, is calculated as

$$KL(P|Q) = \frac{1}{n}\sum_i P(i)\log\frac{P(i)}{Q(i)}. \quad (6)$$

In our case, since Q is uniform, $KL(P|Q) = (n - H_p)/n$, where H_p is the total entropy of distribution P. Note that the larger the KL divergence is, the closer $KL(P|Q)$ approaches to 1 and the worse the security of the AND-tree is.

In summary, the strategy to evaluate the input bias of existing tree structures in the original circuits becomes

- First, evaluate $\Pr_{i\sim I}(i = i^{y^*})$ following Algorithm 1 to determine the upper bound of θ.
- Second, when the upper bound is large enough, do random sampling for circuit primary inputs and then, derive the logic value for the tree input pins, based on which, $KL(P|Q)$ can be calculated following Equation (6). If $KL(P|Q)$ is smaller than a pre-defined threshold, then, we consider the provided security of the tree structure to be large enough.

2) Tree Decomposability Characterization

To characterize the impact of multiple paths to primary outputs, we propose the concept on tree decomposability.

Definition 1 (Decomposable Tree)**.** *An AND-tree structure is decomposable if (1) there exists a path from the internal node of the tree to the primary output that can bypass the root of the tree; and (2) change of the logic value of the internal node can be observed at the primary output through the path.*

Both of the conditions are important. For example, the AND-tree structure in Fig. 7(b) is decomposable because the internal node $Node_1$ can bypass the root of the tree PO_2 and get observed at the output PO_1. Tree decomposability is undesired because it enables the attacker to first de-camouflage the sub-tree structure rooted at $Node_1$, and then de-camouflage the remaining part of the tree, which is also an AND-tree structure, but with fewer input pins. The number of input vectors needed to de-camouflage the decomposable AND-tree is thus limited the sum of the input vectors needed to de-camouflage the two subtrees. Due to tree decomposability, the size of the two subtrees are much smaller than the original AND-tree, which indicates much smaller de-camouflaging complexity.

To determine whether an AND-tree is decomposable, we propose the algorithm shown in Algorithm 2. We traverse the tree structure in a reverse topological order starting from the root. For each internal node u of the tree, if it has more than 1 successors, then, we do a depth-first search starting from u and keep record of all the paths from u to the primary outputs. If the tree root exists in each path, then, the tree is non-decomposable.

Algorithm 2 Determine whether an AND-tree is decomposable

// G is the original circuit and G_t is the AND-tree
// r_t is the root of the tree
$U \leftarrow$ TOPOLOGICALSORT(r, G_t);
for $u \in U$ **do**
$\quad$ **if** $u.\text{fanout} > 1$ **then**
$\quad\quad \{p_1, \ldots, p_m\} \leftarrow$ DFS(u, G);
$\quad\quad$ **if** $\exists i$, s.t. $r \notin p_i$ **then**;
$\quad\quad\quad$ **return** True;
return False;

VI. PROVABLY SECURE IC CAMOUFLAGING

In this section, we will leverage the proposed camouflaging cell generation method and the AND-tree structure to provide provably secure camouflaging strategy. The overall flow of the proposed IC camouflaging framework is illustrated in Fig. 9. The first step is the camouflaging cell library generation with the proposed techniques described in Section IV. Then, accurate characterization is performed to determine the timing, power and area overhead for each cell in the camouflaging cell library. In the third step, existing AND-tree structure is detected for the original netlist. If the pre-defined de-camouflaging complexity is not satisfied, new AND-tree structure needs to be inserted as in the fourth step. Otherwise, we can simply camouflaged the AND-tree structure to enforce the resilience to structural attacks. In the fifth step, we leverage the inserted AND-tree structure to protect all the primary outputs to ensure that at least one large AND-tree exists in the fanin cone of each primary output. We further camouflage the AND-tree structure to enhance the resilience against tree removal attack in the sixth step. After the sixth step, a camouflaged netlist will be generated.

A. AND-Tree Detection in Original Netlist

AND-tree represents a set of circuit structures. We denote all the circuit structures that generate 1 as output for only one input vector as AND-tree and those that generate 0 as output for only one input vector as OR-tree. The pseudo code of the algorithm we propose to detect the tree structure is shown in Algorithm 3. We start from the primary inputs of the circuit and sort all the circuit nodes in a topological order (line 2). For each node, we keep record of the tree rooted at this node by recording the input pins of the tree. For primary inputs, the type of tree rooted at the node can be treated as either AND-type or OR-type (lines 4–6). For the internal nodes, to determine the input pins of the tree structure, we consider the gate type of the node and its predecessors in

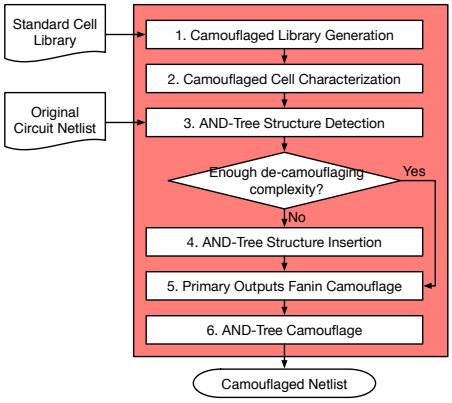

Fig. 9: The proposed IC camouflaging flow.

the circuit graph. Depending on the type of the gate, there are following possibilities (lines 7–31):

- If the gate is INV or BUF, the node will have the same tree as its input (lines 8–10). For INV, function INVERT() is called to change the tree type from AND-type to OR-type or vice versa.
- If the gate is AND or OR, the tree type rooted at the node can first be determined (lines 12–16). Then, to determine the input pins, there are two possible situations depending on the predecessors' tree types and the tree type of the node. When the tree types are the same, larger tree structure can be formed (lines 18–19). In this case, function ADD() is called to add the predecessor's tree structure to the node. When the tree types are different, only the predecessor itself can be added to the tree (lines 20–22).
- If the gate is NAND or NOR, we can treat it as an AND or OR connected with INV and follow the procedure above.
- For other type of gates, including XOR, XNOR, MUX and so on, no tree structure can be formed and the node itself is added to the tree (lines 24–27).

We now use an example to illustrate the Algorithm 3.

Example VI.1. *Consider the circuit shown in Fig. 10(a). As in Fig. 10(b), for primary input* $Node_1$*, the tree type is* ANY *and the input of the tree is* $\{Node_1\}$*. For internal node* $Node_5$*, since it is connected with* $Node_1$ *through a BUF, the tree type for* $Node_5$ *is also* ANY *and the inputs is also* $\{Node_1\}$*. For* $Node_8$*, since it is connected with an XOR gate, the tree type becomes* ANY *and the inputs to the tree is the node itself, i.e.* $\{Node_8\}$*. Consider* $Node_7$*, since it is connected with an OR gate, the tree type has to be* OR*. For the two inputs, i.e.* $Node_5$ *and* $Node_2$*, since the tree types for both nodes are* ANY*, they can be combined to form large tree structure. Therefore, the input pins for the tree rooted at* $Node_7$ *becomes* $\{Node_1, Node_2\}$*. Similarly, we can determine the tree type and tree inputs for* $Node_9$*. Because* $Node_9$ *is connected with an NOR gate, the tree type becomes* AND*.*

After the calculation of the tree structure rooted at each node, we can examine whether the pre-defined de-camouflaging complexity is satisfied as described in Section V-B. If the requirement is not satisfied, new tree structures need to be inserted. In our paper, we do not consider combining existing trees in original netlists with the inserted new trees. Instead, we insert a new tree structure that is able to provide sufficient security by itself.

B. Stochastic Greedy AND-Tree Insertion

The insertion of the AND-tree structure needs to satisfy the following requirements:

- The functionality of the original circuit is not changed.
- The overhead induced by the insertion should be minimized.

Algorithm 3 Algorithm of And-Tree Detection

```
1: Let {AND, ANY, OR} denote a set of tree types.
2: U ← TopologicalSort(G);
3: for u ∈ U do
4:     if u is primary input then
5:         u.treetype ← ANY;
6:         u.treeinput ← u;
7:     else
8:         if u.gatetype ∈ {BUF, INV} then
9:             u.treetype ← u.fanin.treetype;
10:            u.treeinput ← u.fanin.treeinput;
11:        else if u.gatetype ∈ {AND, NAND, OR, NOR} then
12:            if u.gatetype ∈ {AND, NAND} then
13:                u.treetype ← AND;
14:            else if u.gatetype ∈ {OR, NOR} then
15:                u.treetype ← OR;
16:            for v ∈ u.fanin do
17:                if v.treetype = u.treetype and Size(v.fanout) = 1 then
18:                    u.treeinput.Add(v.treeinput);
19:                else
20:                    u.treeinput.Add(v);
21:        else
22:            u.treetype ← ANY;
23:            u.treeinput ← u;
24:        if u.gatetype ∈ {INV, NOR, NAND} then
25:            u.treetype ← Invert(u.treetype);
26: return U.
```

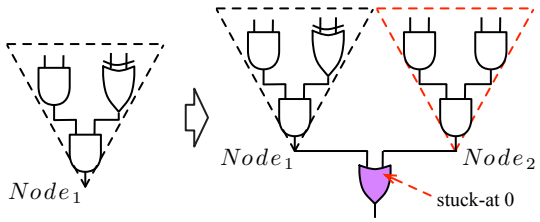

Fig. 11: Insert AND-type tree structure to the circuit ($Node_2$ is stuck-at-0 to guarantee the functional correctness).

- A false interpretation of the AND-tree functionality leads to erroneous outputs.

To satisfy the first requirement, we leverage the STF-type camouflaging cells as described in Section IV. Consider an example circuit as shown in Fig. 11. To insert an AND-tree structure at $Node_1$, we first insert an OR gate to $Node_1$ with the other input $Node_2$ as dummy pin. Then, an AND-tree structure is created with $Node_2$ being the root. The input pins of the AND-tree structure are connected to the primary inputs and camouflaged with XOR-type cells.

To detect the stuck-at 0 fault at $Node_2$, we again follow the same analysis as in Section V. The logic value of $Node_2$, which is 0 in reality, can be expressed as

$$c_y(i) = g_{n+1}(g_1(i_1) \wedge g_2(i_2) \wedge \ldots \wedge g_n(i_n)).$$

Note that $g_{n+1}(i) = 0$ indicates there is a stuck-at-0 fault at $Node_2$, and $g_{n+1}(i) = i$ otherwise. Among all the possible configurations, there are 2^n correct configurations with g_{n+1} interpreted as stuck-at-0 and 2^n incorrect configurations with $g_{n+1}(i) = i$. For any false configuration y, c_y outputs 1 for exactly one input vector, denoted as i^y, and thus, is different from c_{y^*} for exactly one input vector. For the corresponding

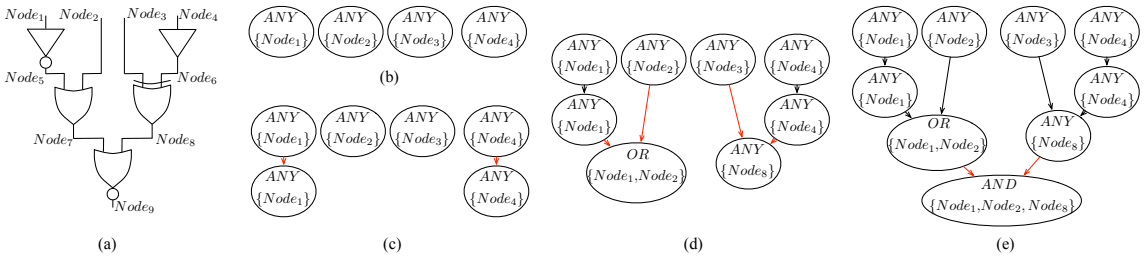

Fig. 10: Detect tree structure in topological order: (a) circuit netlist; (b) (c) (d) (e) start from primary inputs to calculate tree structure in topological order.

indicator function, e_{c_y} is different from $e_{c_{y^*}}$ at exactly two points, i.e. $\{(i^y, 1), (i^y, 0)\}$. Therefore, $\forall y$ with $c_y \neq c_{y^*}$, we have

$$\begin{aligned} &\mathrm{er}_{(i,o)\sim I\times O}(e_{c_y}, e_{c_{y^*}}) \\ =& \Pr_{(i,o)\sim I\times O}[e_{c_y}(i,o) \neq e_{c_{y^*}}(i,o)] \\ =& \Pr_{(i,o)\sim I\times O}[(i,o) \in \{(i^y,0),(i^y,1)\}] \\ =& \Pr_{i\sim I}[i = i^y]. \end{aligned} \tag{7}$$

Since we connect the input pins of the inserted tree structure with circuit primary inputs, we can assume no input bias for tree inputs, which indicates

$$\Pr_{i\sim I}[i = i^y] = \frac{1}{2^n}.$$

Similar to proof in Section V-A, if we set $\epsilon = \frac{1}{2^n}$, then, we have $E_\epsilon = E_C$ and $\mathrm{DIS}(E_\epsilon) = I \times O$. In this case, $\theta = 2^n$. Therefore, $m(e_{c_{y^*}}, E_C) = \mathcal{O}(2^n)$.

Therefore, the required number of input vectors to de-camouflage the circuit increases exponentially to the size of the inserted AND-tree structure. The insertion of OR-tree follows the same procedure except that we need to use an AND gate with stuck-at-1 fault at the dummy input, which is the root of the OR-tree structure.

Algorithm 4 Algorithm of Stochastic Greedy AND-Tree Insertion

```
U_PO ← POs;
U ← TopologicalSort(G);
RemoveCriticalNode(U);
while U_PO ≠ ∅ do
    for u ∈ U do
        u.score ← ComputeIS(G);
    U_IS ← FindTopK(U);
    u_c ← RandomSelectCand(U_IS);
    G ← AndTreeInsert(u_c, G);
    U_PO ← RemoveCoveredPO(U_PO, u_c);
return U;
```

To determine the location for the insertion of the tree structure, we propose a stochastic greedy tree insertion algorithm as shown in Algorithm 4, which tries to minimize the performance overhead and guarantee the functionalities for all primary outputs are protected. We first add all the primary outputs that we hope to protect in a set U_{PO}. Then, to decide the candidate circuit node for tree insertion, we traverse the circuit graph in a topological order and calculate an insertion score (IS) for each internal nodes. IS is defined to consider the node's switching probability SA, observe probability P_{ob} and the number of primary outputs N_O that have not been camouflaged in its fanout cone, which is calculated as

$$IS = \frac{\alpha \times SA - \beta \times P_{ob}}{N_O}. \tag{8}$$

By defining IS following Equation (8), we look for the circuit node with lowest average cost to camouflage one primary output. Here, cost is defined considering introduced power overhead SA and error observability P_{ob}. α and β are coefficients defined to balance SA and P_{ob}. By increasing α, we can reduce the introduced power overhead, while by increasing β, we prefer circuit nodes which leads to better error probability at primary outputs. Note that before we calculate the score, all the circuit nodes along timing critical paths are removed first to guarantee negligible impact on performance. Then, we find k nodes with smallest scores from U and randomly select one node as the candidate for tree insertion. All the primary outputs in the fanout cone of the candidate node are removed from U_{PO} and the procedure is continued until all the primary outputs are protected.

The insertion of AND-tree structure helps camouflage the functionality of original netlist. While the timing overhead can be small since the nodes along critical paths are not changed, the introduced power and area overhead cannot be avoided. However, the size of the inserted tree only depends on the required security level and is independent of the size of original netlist. Meanwhile, while the induced area and power overhead increases linearly as the tree size, the de-camouflaging complexity increases exponentially. Therefore, to ensure certain de-camouflaging complexity, the overhead is acceptable. For relatively large circuit, the overhead is even negligible.

More importantly, the de-camouflaging complexity, which is defined as the number of input-output patterns required for de-camouflaging, is independent of the way that a SAT-problem is formulated and the software package or computer configuration that the attack is carried on. Therefore, the proposed camouflaging framework is provably secure provided that the requirement on the size of non-decomposable tree and input bias is satisfied.

C. AND-Tree Camouflaging Against Removal Attack

By inserting AND-tree into original circuit netlists, the de-camouflaging complexity can be increased exponentially, which ensures good resilience against SAT-based attack. However, because large AND-tree is a unique structure that does not usually exist in general circuit netlist, it is possible for the attacker to identify and remove it. In [29], the authors propose to identify the AND-tree by calculating the signal probability skew (SPS) for each circuit node. SPS of a signal s is defined as $\Pr[s = 1] - 0.5$. In Fig. 12, we use an example to illustrate the attack process. Starting from primary inputs, the attacker traverses the circuit netlist topologically. For a standard cell, the signal probability can be easily calculated while for a camouflaging cell, because its actual functionality in the circuit is unknown, the attacker assumes same probability for each functionality, and calculate the signal probability as the average value. For a signal with large uncertainty, its SPS tends to approach 0. For the root of an AND-tree, its SPS approaches to -0.5 exponentially with respect to the size of the AND-tree. This makes it possible for the attacker to identify the inserted tree structure by SPS.

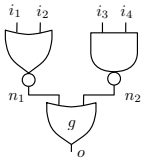

$$SPS(i_1) = SPS(i_2) = SPS(i_3) = SPS(i_4) = 0$$

$$SPS(n_1) = \frac{1}{2} \times \frac{1}{2} - \frac{1}{2} = -\frac{1}{4},\ SPS(n_2) = 1 - \frac{1}{2} \times \frac{1}{2} - \frac{1}{2} = \frac{1}{4}$$

When g is OR gate:

$$SPS(o) = 1 - \frac{1}{4} \times \frac{3}{4} - \frac{1}{2} = \frac{5}{16}$$

When g is XOR-type OR gate:

$$SPS(o) = \frac{1}{2}(1 - \frac{1}{4} \times \frac{3}{4}) + \frac{1}{2}(\frac{1}{4} \times \frac{3}{4}) - \frac{1}{2} = 0$$

Fig. 12: SPS based functional attack: when g is OR gate, $SPS(o) = \frac{5}{16}$ and when g is XOR-type camouflaging cell, whether g works as an OR gate or a NOR gate are equally possible for the attacker [29], and thus $SPS(o) = 0$.

Besides the SPS-based attack, because a non-decomposable AND-tree is an isolated structure that does not have many connections with the original circuit, the attackers can also leverage this structural footprint to detect the inserted AND-tree structure. To protect the inserted AND-tree from such removal attack, we propose to camouflage the structure both functionally and structurally.

We use the example in Fig. 13 to illustrate our AND-tree camouflaging strategy. Consider an 8-input AND-tree in Fig. 13(a). We first replace the standard cells in the AND-tree with camouflaging cells that look the same and share the same functionality, as in Fig. 13(b). Then, we replace the NAND, NOR and INV cells with XOR-type camouflaging cells that look differently but share the same functionality, as in Fig. 13(c). Because the attacker cannot determine whether the output of each cell in the AND-tree is negated or not, e.g. whether an AND cell works as an AND or a NAND cell in the circuit, the SPS for each node in the AND-tree is always kept as 0 according to [29]. Therefore, functional attacks by SPS are rendered useless.

To prevent removal attack based on structural information, we leverage the STF-type camouflaging cell to connect the internal nodes of the AND-tree to other gates as in Fig. 13(d). For a $\tilde{n}$-input AND-tree, there are in total $\tilde{n} - 1$ gates in the tree following the structure in Fig. 13(a). To ensure the size of the largest AND-tree detected by the attacker to be less than $\tilde{n}'$, we can always insert $O((\tilde{n} - 1)/(\tilde{n}' - 1))$ STF-type camouflaging cells to create dummy connections to the internal nodes as in Fig. 13(d). Meanwhile, to prevent the attackers from identifying the inputs to the AND-tree, we can insert extra XOR-type BUF cells to other primary inputs. *Note that by inserting dummy connections with STF-type cells, the original circuit functionality is maintained. Meanwhile, the inserted AND-tree is still non-decomposable from the defense perspective since the logic value of AND-tree internal nodes cannot be sensitized through the dummy connections. However, from the attackers' point of view, because he cannot determine the connections are dummy based on structural attack following Algorithm 3, the largest non-decomposable tree that can be detected by structural attack is reduced significantly. At the same time, because structural and functional camouflaging focuses on internal nodes of the tree structure, the input bias is not impacted as well.* Therefore, the resilience to SAT-based attack is not impacted, while the vulnerability to removal attacks is mitigated significantly.

D. Comparison between State-of-the-Art Techniques

Until now, we have described our IC camouflaging strategy that detects, inserts and camouflages AND-tree structure to provide guaranteed security towards SAT-based attack. Similar idea to leverage AND-tree structures has also been explored by Anti-SAT [24] and CamoPerturb [23]. In this section, we compare the three strategies in terms of provided security, overhead and their impact on the original circuit netlist, i.e. whether re-synthesis is required.

Assume an AND-tree with $\tilde{n}$-bit inputs is to be inserted into the circuit. According to Anti-SAT strategy, in fact, two subtrees, denoted as Sub_1 and Sub_2, are inserted into the circuit. Sub_1 and Sub_2 are AND-trees of the same size with $\tilde{n}$ input pins, and share the same input signals. An inverter is inserted at the output of Sub_2. XOR-type BUF cells are inserted at the input pins of the two AND-trees. For the circuit to function correctly, the XOR-type BUF cells of same input signals in the Sub_1 and Sub_2 need to have the same functionality. To de-camouflage the circuit, the attacker always needs to query $2^{\tilde{n}}$ input vectors [24].

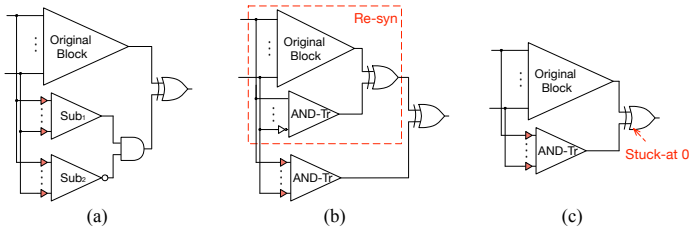

Fig. 14: Comparison on AND-tree insertion strategy: (a) Anti-SAT [24]; (b) CamoPerturb [23]; (c) our insertion strategy.

For CamoPerturb strategy, to insert a $\tilde{n}$-bit AND-tree, a specific input vector i^* is first selected. Then, original circuit is re-synthesized by flipping the output value corresponding to i^*. An AND-tree is then inserted to correct the flipped output just for i^*. XOR-type BUF cells are inserted into the input pins of the AND-tree and their actual functionality in the circuit is determined by i^*. Based on [23], to de-camouflage the circuit, all input vectors are discriminating inputs and for each $i \neq i^*$, at most one false functionality can be pruned. However, it should be noted that i^* can rule out all the false functionalities. Because i^* is unknown to the attackers, on average, $2^{\tilde{n}-1}$ input vectors need to be measured. In the best case, the attacker has to measure $2^{\tilde{n}}$ input vectors to de-camouflage the AND-tree. However, in the worst case, only 1 input vector, i.e. i^* is required for the attacker. It should be noted that for our AND-tree insertion strategy, as shown in TABLE III, the de-camouflaging complexity is also $2^{\tilde{n}}$. This is because with our strategy, the circuit output is never impacted by the AND-tree output due to the stuck-at-0 input pin at the XOR gate. Therefore, for any input vector, exactly one false functionality can be ruled out.

The three strategies mainly introduce area and power overhead while the impact on timing can be negligible by avoiding any modification of circuit critical paths. Compared with our method, Anti-SAT suffers from almost double area and power overhead because one AND-tree and one NAND-tree of the same size is inserted. For CamoPerturb, besides the overhead introduced by the inserted AND-tree, extra overhead can be introduced in the process of re-synthesis. As we show in Section VII-B, large overhead can be introduced in the process of re-synthesis depending on i^*. We summarize the comparison in TABLE III. As we can see, our strategy for AND-tree insertion provides the best security guarantee. Meanwhile, because no re-synthesis is required for our methods, it introduces less modification to the original design and thus is easier for final design closure.

TABLE III: Comparison with CamoPerturb [23] and Anti-SAT [24].

Strategy	De-cam Complexity			Overhead	Resyn
	Worst	Avg	Best		
Ours	$2^{\tilde{n}}$	$2^{\tilde{n}}$	$2^{\tilde{n}}$	$\tilde{n}$-bit tree	No
CamoPerturb	1	$2^{\tilde{n}-1}$	$2^{\tilde{n}}$	$\tilde{n}$-bit tree+ Resyn	Yes
Anti-SAT	$2^{\tilde{n}}$	$2^{\tilde{n}}$	$2^{\tilde{n}}$	2 $\tilde{n}$-bit tree	No

VII. Experimental Results

In this section, we report on our experiments to demonstrate the effectiveness of the proposed IC camouflaging strategy. The camouflaging

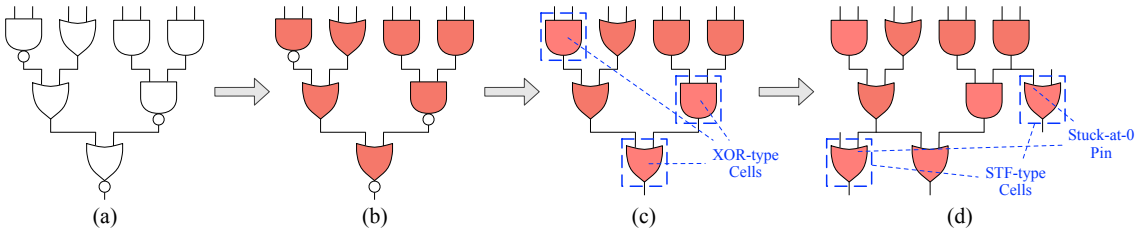

Fig. 13: AND-tree protection: (a) original AND-tree structure; (b) and (c) functional camouflaging to reduce SPS for the root node; (d) structural camouflaging to add dummy connections from AND-tree internal nodes.

TABLE IV: Verify the proposed camouflaging cell generation strategy by de-camouflaging time, attack on individual POs and introduced overhead.

bench	# PI	# PO	# gate	time	partial	area (%)	power (%)
c432	36	7	203	1.758	7/7	2.5	1.9
c880	60	23	466	1.2×10^4	23/23	1.1	0.85
c1355	41	32	619	N/A	29/32	0.86	0.73
c1908	33	25	938	N/A	0/25	0.58	0.71
c2670	233	64	1490	N/A	60/64	0.37	0.41
c3540	50	22	1741	N/A	9/22	0.27	0.13
c5315	178	123	2608	N/A	116/123	0.17	0.11
i4	192	6	536	1.9×10^3	6/6	1.2	0.94
apex2	39	3	652	N/A	1/3	0.77	0.62
ex5	8	63	1126	6.9×10^2	63/63	0.43	0.32
i9	88	63	1186	2.1×10^4	63/63	0.45	0.22
i7	199	67	1581	1.5×10^2	67/67	0.37	0.40
k2	46	45	1906	N/A	24/45	0.21	0.17
dalu	75	16	2373	N/A	3/16	0.21	0.18

algorithm is implemented in C++. The SAT-based de-camouflaging algorithm is adopted from [27] and the SPS-based removal attack is implemented following [29]. We run all the experiments on an eight-core 3.40 GHz Linux server with 32 GB RAM. The benchmarks are chosen from ISCAS and MCNC benchmarks [40], [41]. For the de-camouflaging algorithm, we set the runtime limit to 1.5×10^5 seconds.

A. Verification of Camouflaging Cell Generation Strategy

We first demonstrate the security achieved by using camouflaging cell generation strategy. As described in Section IV-C, we first replace all the standard cells with camouflaging cells and then, randomly change 10 cells with camouflaging cells that appear to be different but work with same functionality. We show the introduced overhead, de-camouflaging complexity and the time required for the SAT-based algorithm to resolve the original circuit functionality in TABLE IV. N/A indicates that the camouflaged netlist cannot be resolved within 1.5×10^5 seconds. As we can see, the area overhead, which is calculated as the sum of the area of each cell, is on average 0.68% and the power overhead is on average 0.55%, both of which are very small even for small benchmark circuits. Meanwhile, for large circuits, simply with the camouflaging cell generation strategy, the de-camouflaging algorithm cannot be finished within the pre-defined time. However, as we have pointed out in Section IV-C, the SAT-based algorithm can still de-camouflage some small benchmarks with less than 1600 gates. Also, for the circuits that cannot be fully de-camouflaged, we can still run de-camouflaging attacks for each primary outputs separately and partially de-camouflage the design as shown in the partial column in TABLE IV. The experimental results demonstrates the effectiveness of the camouflaging cell generation strategy for large circuit, and also shows the necessity to have other SAT-resilient protection strategies.

B. Evaluation of AND-tree based Camouflaging Strategy

To evaluate the security of the AND-tree based camouflaging strategy, we start from stand-alone tree structures. We show the increase of the de-camouflaging complexity and time with respect to the tree size in Fig. 15(a). As we can see, both the de-camouflaging time and complexity increase exponentially as we expect. To examine the impact of tree decomposability, we fix the size of an AND-tree, i.e. 15 input pins, and change the size of the largest non-decomposable subtree in the 15-input AND-tree. The size of other non-decomposable subtrees is limited to be smaller than 3. We show the change of the de-camouflaging time and complexity in Fig. 15(b). As we have discussed in Section V-B2, the de-camouflaging complexity of the 15-input tree is limited by the sum of the de-camouflaging complexity of each subtree. When the size of the largest non-decomposable tree is much larger than the other subtrees, the de-camouflaging complexity of the 15-input tree is mainly determined by its largest non-decomposable subtree. As in Fig. 15(b), the de-camouflaging complexity indeed reduces exponentially with the size of the largest non-decomposable tree. We also verify the impact of input bias. We add extra circuits to the fanin cone of the tree input pins and gradually changes the input number of the extra circuits to change the KL divergence of the input distribution compared to uniform distribution. As we show in Fig. 15(c), with the decrease of the input number of the added circuits in the fanin cone, i.e. the increase of the normalized KL divergence, both the de-camouflaging time and complexity decreases.

TABLE V: Existing tree structure in benchmark circuits.

bench		D-tree	ND-tree	norm KL div.
ISCAS	c1355	7	3	0.7
	c1908	14	12	0.339
	c2670	34	34	0.640
	c3540	10	9	0.671
	c5315	10	9	0.093
MCNC	i4	7	7	0.732
	ex5	6	6	0.589
	i7	4	3	0.612
	k2	175	39	0.968

To further examine the AND-tree structure, we consider the tree structure in the original netlist. We detect the existing AND-tree structure following Algorithm 3; In TABLE V, we list the input size of the largest decomposable tree detected in the original netlist, i.e. D-tree, and the largest detected non-decomposable tree in the original netlist, i.e. ND-tree. For most of the circuits, the existing non-decomposable tree structure is very small. For benchmark c2670 and k2, large tree structure exists. The calculation of normalized KL divergence indicates that high bias exists for the input pins of tree structure in k2 since the value is very close to 1. We camouflage the input pins for tree structures in both benchmarks and use SAT-based method to de-camouflage. For c2670, original circuit functionality cannot be resolved within the pre-defined time threshold, while for k2, the de-camouflaging algorithm finishes within 8.5 seconds and 70 iterations. The results demonstrate the importance to consider both tree decomposability and input bias to evaluate the impact of the AND-tree structure in circuit netlist.

Then, we insert tree structure into the benchmark circuits following Algorithm 4. We set $\alpha = \beta = 1$ for IS evaluation. We show the trade-off between the area overhead and the de-camouflaging time and

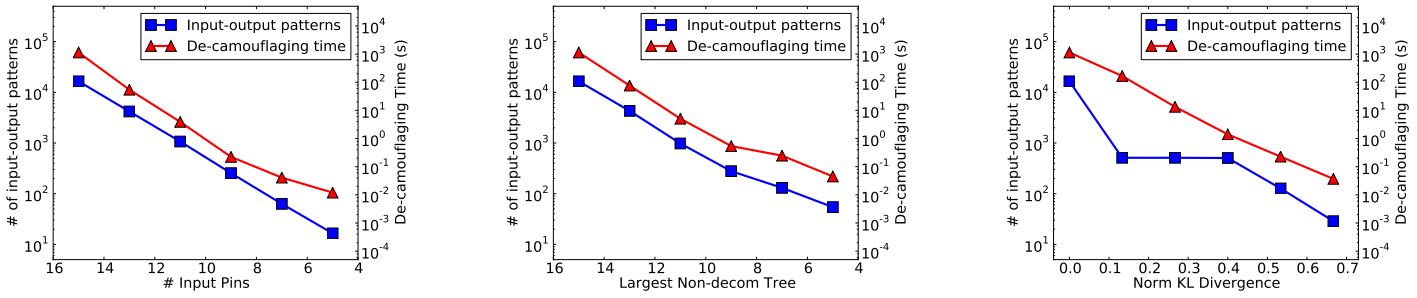

(a) (b) (c)

Fig. 15: Effectiveness of tree structure and impact of tree decomposability and input bias: (a) de-camouflaging complexity and time for ideal AND-tree structure; (b) change of de-camouflaging complexity and time with the size of the largest non-decomposable tree; (c) change of de-camouflaging complexity and time with the input bias.

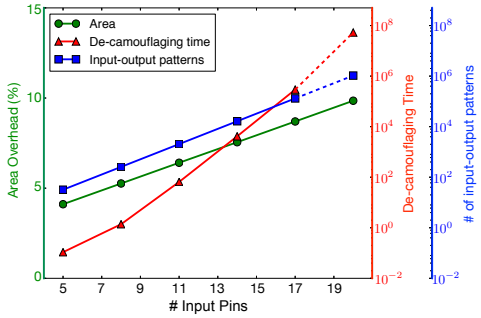

Fig. 16: Trade-off between overhead and de-camouflaging complexity (dotted lines indicate extrapolation).

TABLE VI: Introduced overhead of the tree-based camouflaging strategy when 64-input AND-tree is inserted.

bench	gate	overhead			security	
		area	power	timing	de-cam time	partial
i4	536	32.5	19.4	0.5	N/A	0/6
i9	1186	11.5	6.2	0.1	N/A	0/63
c2670	1490	11.8	6.0	0.1	N/A	0/64
i7	1581	9.7	4.7	0.2	N/A	0/67
dalu	2373	5.5	4.3	0.0	N/A	0/16
c5315	2608	5.9	2.8	0.0	N/A	0/123
c7552	3719	4.8	2.4	0.0	N/A	0/107
des	6729	1.9	1.2	0.0	N/A	0/245

complexity in Fig. 16 for benchmark c880. As we can see, the area overhead increases linearly with respect to the size of inserted tree while the de-camouflaging time and complexity increases exponentially. We then insert 64-input AND-tree structure to benchmark circuits. We leverage SAT-based attack to de-camouflage the camouflaged circuits. We also extract the subcircuits for each primary output and try to resolve the circuit separately. We show the results in TABLE VI. As we can see, SAT-based attack cannot de-camouflage any primary output of each benchmark circuits. We also report the introduced overhead, including power, area and timing in TABLE VI. As shown in TABLE VI, the main overhead comes from area and power while the impact on timing is negligible. Meanwhile, for large circuit, e.g. des, the area and power overhead is less than 2%.

We then compare the proposed tree insertion strategy with Anti-SAT [24] and CamoPerturb proposed in [23]. We use all the three methods to insert 64-bit AND-tree into the benchmark circuits and compare the introduced power and area overhead in TABLE VII. Since analytical comparison on the de-camouflaging complexity is provided in Section

TABLE VII: Area and power overhead comparison with Anti-SAT and CamoPerturb.

bench	Anti-SAT [24]		CamoPerturb [23]		Ours	
	area	power	area	power	area	power
i4	62.2	38.9	49.4	41.6	32.5	19.4
i9	23.4	12.3	29.1	29.6	11.5	6.2
c2670	24.9	12.0	25.8	19.0	15.2	6.0
i7	19.6	9.4	26.3	22.1	9.7	4.7
dalu	11.1	8.6	11.2	9.65	5.5	4.3
c5315	12.6	5.6	16.2	13.3	7.9	2.8
c7552	10.3	4.8	11.9	8.65	6.9	2.4
des	3.67	2.4	11.1	15.7	1.9	1.2

VI-D, we do not run SAT-based attack for the three strategies. As in TABLE VII, our method achieves similar overhead compared with Anti-SAT. CamoPerturb suffers from larger power and area overhead compared with Anti-SAT and our strategy since large overhead is introduced in the re-synthesis process.

C. Impact of Structural and Functional Camouflaging

We now verify the effectiveness of the structural and functional camouflaging for the AND-tree based camouflaging strategy and demonstrate the introduced overhead. We insert AND-tree with 64 input bins. We consider SPS-based methods proposed in [29] as functional attack and tree detection algorithm following Algorithm 2 as structural attack, which represents the state-of-the-art removal attack strategies. As shown in TABLE VIII, after structural and functional camouflaging, the area and power overhead increases on average by 5.1% and 0.3%. However, for large benchmarks, i.e. des, the total area and power overhead after structural and functional camouflaging are less than 3%. After structural and functional camouflaging, SPS for the each internal node of AND-tree becomes 0.0, and the size of the largest non-decomposable AND-tree that can be detected following Algorithm 3 (i.e. "detected AND-tree" in TABLE VIII) is 4. Therefore, structural and functional camouflaging can protect the inserted tree structure against the state-of-the-art removal attack strategies. Meanwhile, as we have discussed in Section VI-C, because the logic value of internal nodes of the AND-tree cannot be observed from the dummy connections, the overall resilience to SAT-attack is not reduced. As shown in TABLE VIII, for the circuit netlists after structural and functional camouflaging, SAT-attack cannot be finished within pre-defined time threshold.

D. Effectiveness of Combination of Two Camouflaging Strategies

Finally, we demonstrate the effectiveness of combining the two camouflaging strategies, i.e. camouflaging cell generation strategy and AND-tree based camouflaging strategy. To combine the two camouflaging strategies, we first insert an AND-tree structure into the original netlist following Algorithm 4. Then, we leverage the XOR-type and STF-type

TABLE VIII: Verification of overhead and effectiveness of structural and functional camouflaging.

bench	ICCAD 2016 [14]					Ours				
	area (%)	power (%)	SPS	detected ND-tree	SAT-attack	area (%)	power (%)	SPS	detected ND-tree	SAT-attack
i4	32.5	19.4	0.5	64	N/A	46.8	20.3	0.0	4	N/A
i9	11.5	6.2	0.5	64	N/A	16.4	6.5	0.0	4	N/A
c2670	15.2	6.0	0.5	64	N/A	19.1	6.3	0.0	4	N/A
i7	9.7	4.7	0.5	64	N/A	13.7	4.9	0.0	4	N/A
dalu	5.5	4.3	0.5	64	N/A	7.8	4.5	0.0	4	N/A
c5315	7.9	2.8	0.5	64	N/A	9.8	2.9	0.0	4	N/A
c7552	6.9	2.4	0.5	64	N/A	8.3	2.5	0.0	4	N/A
des	1.9	1.2	0.5	64	N/A	2.6	1.3	0.0	4	N/A

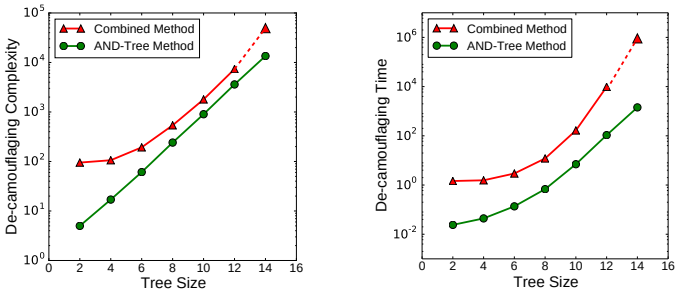

(a) (b)

Fig. 17: Verification of effectiveness of combining the proposed two camouflaging techniques on benchmark c880 (dotted line indicate extrapolation).

cells to further camouflage the circuit netlists following the strategy described in Section IV-C. We examine the effectiveness of the combined strategy by comparing the de-camouflaging complexity and time with the situation when only AND-tree based strategy is used. We run the experiments on benchmark c880. As shown in Fig. 17, by combining the two camouflaging strategies, both the de-camouflaging complexity and time are further increased, which indicates better security level.

VIII. Conclusion

In this paper, we have proposed a quantitative security criterion for de-camouflaging complexity measurements. The security criterion was formally analyzed based on the equivalence between the de-camouflaging strategy and the active learning scheme. Meanwhile, two camouflaging techniques were proposed: the low-overhead camouflaging cell library and the AND-tree structure, following the security criterion. A provably secure camouflaging framework was then developed to combine the two techniques, which achieves exponentially increasing security levels at the cost of linearly increasing overhead. Experimental results using the security criterion demonstrated that the camouflaged circuits with the proposed framework achieve high resilience against the SAT-based attack with only negligible performance overhead.

References

[1] Y. Jin, "Introduction to hardware security," *Electronics*, vol. 4, no. 4, pp. 763–784, 2015.

[2] P. Subramanyan, N. Tsiskaridze, W. Li, A. Gascon, W. Y. Tan, A. Tiwari, N. Shankar, S. Seshia, and S. Malik, "Reverse engineering digital circuits using structural and functional analyses," *IEEE Trans. on Emerging Topics in Computing*, vol. 2, no. 1, pp. 63–80, 2014.

[3] S. E. Quadir, J. Chen, D. Forte, N. Asadizanjani, S. Shahbazmohamadi, L. Wang, J. Chandy, and M. Tehranipoor, "A survey on chip to system reverse engineering," *ACM J. on Emerging Technologies in Computing Systems*, vol. 13, no. 1, pp. 6:1–6:34, 2016.

[4] R. Torrance and D. James, "The state-of-the-art in semiconductor reverse engineering," in *Proc. IEEE/ACM Design Automation Conf.*, 2011, pp. 333–338.

[5] T. Meade, Z. Zhao, S. Zhang, D. Z. Pan, and Y. Jin, "Revisit sequential logic obfuscation: Attacks and defenses," in *Proc. IEEE Int. Symp. on Circuits and Systems*, 2017.

[6] "Chipwork," http://ww.chipworks.com/.

[7] G. T. Becker, F. Regazzoni, C. Paar, and W. P. Burleson, "Stealthy dopant-level hardware trojans: extended version," *J. of Cryptographic Engineering*, vol. 4, no. 1, pp. 19–31, 2014.

[8] L.-W. Chow, W. M. Clark Jr, and J. P. Baukus, "Covert transformation of transistor properties as a circuit protection method," May 15 2007, US Patent 7,217,977.

[9] L.-W. Chow, J. P. Baukus, and W. M. Clark Jr, "Integrated circuits protected against reverse engineering and method for fabricating the same using an apparent metal contact line terminating on field oxide," Nov. 13 2007, US Patent 7,294,935.

[10] J. Rajendran, M. Sam, O. Sinanoglu, and R. Karri, "Security analysis of integrated circuit camouflaging," in *Proc. ACM Conf. on Computer & Communications Security*, 2013, pp. 709–720.

[11] R. P. Cocchi, J. P. Baukus, L. W. Chow, and B. J. Wang, "Circuit camouflage integration for hardware IP protection," in *Proc. IEEE/ACM Design Automation Conf.*, 2014, pp. 153:1–153:5.

[12] A. Chen, X. S. Hu, Y. Jin, M. Niemier, and X. Yin, "Using emerging technologies for hardware security beyond PUFs," in *Proc. Design, Automation and Test in Europe*, March 2016, pp. 1544–1549.

[13] T. Winograd, H. Salmani, H. Mahmoodi, K. Gaj, and H. Homayoun, "Hybrid STT-CMOS designs for reverse-engineering prevention," in *Proc. IEEE/ACM Design Automation Conf.*, 2016, pp. 88:1–88:6.

[14] M. Li, K. Shamsi, T. Meade, Z. Zhao, B. Yu, Y. Jin, and D. Z. Pan, "Provably secure camouflaging strategy for IC protection," in *Proc. Int. Conf. on Computer Aided Design*, 2016, pp. 28:1–28:8.

[15] K. Shamsi, M. Li, T. Meade, Z. Zhao, D. Z. Pan, and Y. Jin, "Circuit obfuscation and oracle-guided attacks: Who can prevail?" in *Proc. IEEE Great Lakes Symp. on VLSI*, 2017.

[16] A. Vijayakumar, V. C. Patil, D. E. Holcomb, C. Paar, and S. Kundu, "Physical design obfuscation of hardware: A comprehensive investigation of device and logic-level techniques," *IEEE Trans. on Information Forensics and Security*, vol. 12, no. 1, pp. 64–77, 2017.

[17] S. Malik, G. T. Becker, C. Paar, and W. P. Burleson, "Development of a layout-level hardware obfuscation tool," in *Proc. IEEE Annual Symp. on VLSI*, 2015, pp. 204–209.

[18] A. Iyengar and S. Ghosh, "Threshold voltage-defined switches for programmable gates," *GOMACTech*, 2016.

[19] B. Erbagci, C. Erbagci, N. E. C. Akkaya, and K. Mai, "A secure camouflaged threshold voltage defined logic family," in *Proc. IEEE Int. Symp. on Hardware Oriented Security and Trust*, 2016, pp. 229–235.

[20] M. I. M. Collantes, M. El Massad, and S. Garg, "Threshold-dependent camouflaged cells to secure circuits against reverse engineering attacks," in *Proc. IEEE Annual Symp. on VLSI*. IEEE, 2016, pp. 443–448.

[21] Y. W. Lee and N. A. Touba, "Improving logic obfuscation via logic cone analysis," in *Proc. IEEE Latin-American Test Symp.*, 2015, pp. 1–6.

[22] K. Shamsi, M. Li, T. Meade, Z. Zhao, D. Z. Pan, and Y. Jin, "Cyclic obfuscation for creating sat-unresolvable circuits," in *Proc. IEEE Great Lakes Symp. on VLSI*, 2017.

[23] M. Yasin, B. Mazumdar, O. Sinanoglu, and J. Rajendran, "CamoPerturb: Secure IC camouflaging for minterm protection," in *Proc. Int. Conf. on Computer Aided Design*, 2016, pp. 29:1–29:8.

[24] Y. Xie and A. Srivastava, "Mitigating SAT attack on logic locking," in *Proc. Int. Conf. on Cryptographic Hardware and Embedded Systems*, 2016, pp. 127–146.

[25] M. Yasin, B. Mazumdar, J. Rajendran, and O. Sinanoglu, "SARLock: SAT attack resistant logic locking," in *Proc. IEEE Int. Symp. on Hardware Oriented Security and Trust*, 2016, pp. 236–241.

[26] M. El Massad, S. Garg, and M. V. Tripunitara, "Integrated circuit (IC) decamouflaging: Reverse engineering camouflaged ICs within minutes." in *Proc. Network and Distributed System Security Symp.*, 2015.
[27] P. Subramanyan, S. Ray, and S. Malik, "Evaluating the security of logic encryption algorithms," in *Proc. IEEE Int. Symp. on Hardware Oriented Security and Trust*, 2015, pp. 137–143.
[28] C. Yu, X. Zhang, D. Liu, M. Ciesielski, and D. Holcomb, "Incremental SAT-based reverse engineering of camouflaged logic circuits," *IEEE Trans. on Computer-Aided Design of Integrated Circuits and Systems*, vol. PP, no. 99, pp. 1–1, 2017.
[29] M. Yasin, B. Mazumdar, O. Sinanoglu, and J. Rajendran, "Security analysis of Anti-SAT," in *Proc. Asia and South Pacific Design Automation Conf.*, 2017.
[30] S. Dasgupta and J. Langford, "A tutorial on active learning," in *Proc. Int. Conf. on Machine Learning*, 2009.
[31] D. Cohn, L. Atlas, and R. Ladner, "Improving generalization with active learning," *J. of Machine learning*, vol. 15, no. 2, pp. 201–221, 1994.
[32] S. Hanneke, "A bound on the label complexity of agnostic active learning," in *Proc. Int. Conf. on Machine Learning*, 2007, pp. 353–360.
[33] J. Rajendran, O. Sinanoglu, and R. Karri, "VLSI testing based security metric for IC camouflaging," in *Proc. IEEE Int. Test Conf.*, 2013, pp. 1–4.
[34] K. Shamsi, M. Li, T. Meade, Z. Zhao, D. Z. Pan, and Y. Jin, "AppSAT: Approximately deobfuscating integrated circuits," in *Proc. IEEE Int. Symp. on Hardware Oriented Security and Trust*, 2017.
[35] R. Wiener, "An algorithm for learning boolean functions for dynamic power reduction," Ph.D. dissertation, University Of Haifa, 2007.
[36] "NanGate FreePDK45 Generic Open Cell Library," http://www.si2.org/openeda.si2.org/projects/nangatelib, 2008.
[37] Mentor Graphics, "Calibre verification user's manual," 2008.
[38] "Predictive Technology Model ver. 2.1," http://ptm.asu.edu, 2008.
[39] S. Kullback, *Information theory and statistics*. Courier Corporation, 1968.
[40] F. Brglez, D. Bryan, and K. Kozminski, "Combinational profiles of sequential benchmark circuits," in *Proc. IEEE Int. Symp. on Circuits and Systems*, 1989, pp. 1929–1934.
[41] S. Yang, "Logic synthesis and optimization benchmarks user guide: Version 3.0," MCNC Technical Report, Tech. Rep., 1991.

Meng Li received his B.S. degree in Microelectronics from Peking University, Beijing, China in 2013. He is currently pursuing the Ph.D degree in Electrical and Computer Engineering, University of Texas at Austin, under the supervision of Prof. David Z. Pan. His research interests include hardware-oriented security, reliability, power grid simulation acceleration and deep learning. He received best paper award in HOST 2017 and Graduate Fellowship from UT Austin in 2013.

Kaveh Shamsi (S'15) received the B.S. degree in Electrical Engineering from the Sharif University of Technology, Tehran, Iran, in 2014. He is currently pursuing a Ph.D. degree in Computer Engineering at the University of Florida Florida, Gainesville, USA under the supervision of Dr. Yier Jin. His research focuses on using analog and digital circuit design, and formal methods to advance hardware security. He is the recipient of the HOST 2017 best paper award.

Travis Meade recieved his B.S. degree in Mathematics from University of Central Florida, Orlando, Florida, United States of America in 2012. He is currently pursuing a Ph.D. degree in Computer Science at University of Central Florida under the supervision of Dr. Shaojie Zhang and Dr. Yier Jin. His research focuses on using computer algorithms of annotating gate-level netlists. He received best paper award in ASP-DAC 2016 and HOST 2017.

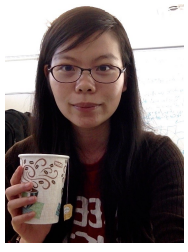

Zheng Zhao recieved his B.S. degree in Automation from Tongji University, Shanghai, China in 2012 and M.S in Electrical and Computer Engineering from Shanghai Jiao Tong University, Shanghai, China in 2015. She is currently pursuing the Ph.D degree in Electrical and Computer Engineering, University of Texas at Austin, under the supervision of Prof. David Z. Pan. Her research interests include hardware security, optical computing/interconnect and logic synthesis.

Bei Yu (S'11–M'14) received his Ph.D. degree from the Department of Electrical and Computer Engineering, University of Texas at Austin in 2014. He is currently an Assistant Professor in the Department of Computer Science and Engineering, The Chinese University of Hong Kong. He has served in the editorial boards of Integration, the VLSI Journal and IET Cyber-Physical Systems: Theory & Applications. He received four Best Paper Awards at International Symposium on Physical Design 2017, SPIE Advanced Lithography Conference 2016, International Conference on Computer Aided Design 2013. and Asia and South Pacific Design Automation Conference 2012, plus three additional Best Paper Award nominations at DAC/ICCAD/ASPDAC, and three ICCAD contest awards in 2015, 2013 and 2012.

Yier Jin is currently an assistant professor in the EECS Department at the University of Central Florida. He received his PhD degree in Electrical Engineering in 2012 from Yale University after he got his B.S. and M.S. degrees in Electrical Engineering from Zhejiang University, China, in 2005 and 2007, respectively.

His research focuses on the areas of trusted embedded systems, trusted hardware intellectual property (IP) cores and hardware-software co-protection on computer systems. He proposed various approaches in the area of hardware security, including the hardware Trojan detection methodology relying on local side-channel information, the post-deployment hardware trust assessment framework, and the proof-carrying hardware IP protection scheme. He is also interested in the security analysis on Internet of Things (IoT) and wearable devices with particular emphasis on information integrity and privacy protection in the IoT era. He is awarded the DoE Early CAREER Award in 2016 and is the best paper award recipient of DAC'15, ASP-DAC'16, and HOST'17.

David Z. Pan (S'97-M'00-SM'06-F'14) received his B.S. degree from Peking University, and his M.S. and Ph.D. degrees from University of California, Los Angeles (UCLA). From 2000 to 2003, he was a Research Staff Member with IBM T. J. Watson Research Center. He is currently the Engineering Foundation Professor at the Department of Electrical and Computer Engineering, The University of Texas at Austin. His research interests include cross-layer nanometer IC design for manufacturability, reliability, security, physical design, analog design automation, and CAD for emerging technologies such as 3D-IC and nanophotonics. He has published over 280 technical papers, and is the holder of 8 U.S. patents. He has graduated 21 PhD students who are now holding key academic and industry positions.

He has served as a Senior Associate Editor for ACM Transactions on Design Automation of Electronic Systems (TODAES), an Associate Editor for IEEE Transactions on Computer Aided Design of Integrated Circuits and Systems (TCAD), IEEE Transactions on Very Large Scale Integration Systems (TVLSI), IEEE Transactions on Circuits and Systems PART I (TCAS-I), IEEE Transactions on Circuits and Systems PART II (TCAS-II), IEEE Design & Test, Science China Information Sciences, Journal of Computer Science and Technology, IEEE CAS Society Newsletter, etc. He has served in the Executive and Program Committees of many major conferences, including DAC, ICCAD, ASPDAC, and ISPD. He is the ASPDAC 2017 Program Chair, ICCAD 2018 Program Chair, DAC 2014 Tutorial Chair, and ISPD 2008 General Chair.

He has received a number of awards for his research contributions, including the SRC 2013 Technical Excellence Award, DAC Top 10 Author in Fifth Decade, DAC Prolific Author Award, ASP-DAC Frequently Cited Author Award, 14 Best Paper Awards at premier venues (HOST 2017, SPIE 2016, ISPD 2014, ICCAD 2013, ASPDAC 2012, ISPD 2011, IBM Research 2010 Pat Goldberg Memorial Best Paper Award, ASPDAC 2010, DATE 2009, ICICDT 2009, SRC Techcon in 1998, 2007, 2012 and 2015) plus 11 additional Best Paper Award nominations at DAC/ICCAD/ASPDAC/ISPD, Communications of the ACM Research Highlights (2014), ACM/SIGDA Outstanding New Faculty Award (2005), NSF CAREER Award (2007), SRC Inventor Recognition Award three times, IBM Faculty Award four times, UCLA Engineering Distinguished Young Alumnus Award (2009), UT Austin RAISE Faculty Excellence Award (2014), and many international CAD contest awards, among others. He is a Fellow of IEEE and SPIE.